Journal of Nuclear Materials 390–391 (2009) 392–394

Contents lists available at ScienceDirect

Journal of Nuclear Materials

journal homepage: www.elsevier.com/locate/jnucmat

Interpretive modelling of scrape-off plasmas on the MAST tokamak

J. Harrison [a,b,*], S. Lisgo [a], G.F. Counsell [c], K. Gibson [b], J. Dowling [a], L. Trojan [d], D. Reiter [e]

[a] Euratom/UKAEA Fusion Association, Culham Science Centre, D2/2.01 Fusion Association, Abingdon, Oxfordshire OX14 3DB, UK
[b] University of York, Heslington, York, UK
[c] Fusion for Energy, Barcelona, Spain
[d] The University of Manchester, Oxford Road, Manchester, UK
[e] IPP, Forschungszentrum Juelich GmbH, EURATOM Association, D-52425 Juelich, Germany

ARTICLE INFO

PACS:
52.55.Fa
52.65.Kj

ABSTRACT

Electrical currents in the scrape-off layer (SOL) of MAST are modelled using an interpretive Onion-Skin Model (OSM) constrained with experimental data from MAST diagnostics. The model was extended to include the effects of the magnetic mirror force, which has a strong influence on the particle and momentum balance in spherical tokamaks, such as MAST [1]. These modifications serve to more accurately model the parallel electric fields present in the MAST SOL, which can alter plasma dynamics via the $E \times B$ drift. Simulations show that the electrical current at the divertor targets is predominantly thermoelectric, whereas Pfirsch–Schlüter currents have a greater contribution to the total current in the bulk of the SOL plasma.

1. Introduction

The scrape-off layer (SOL) of the MAST tokamak was modelled using an interpretive Onion-Skin Model (OSM) [2], which solves 1-D fluid equations for momentum and particle conservation along magnetic flux tubes. Experimental data is input into the code from diagnostics on MAST in the form of boundary conditions and to place constraints on the plasma solution. In this case, plasma density and temperature information at the midplane and divertor targets was provided by Thomson scattering and Langmuir probes respectively. Information about the magnetic geometry of MAST was obtained from the EFIT code in order to generate the grid to input into the code and to model the effects of magnetic mirror force terms in the particle and momentum conservation equations, which are proportional to $\nabla_{\parallel} B / B$. It has been shown that the magnetic mirror force strongly influences the boundary plasma in spherical tokamaks [1], affecting density and, to a lesser extent, temperature profiles along magnetic flux tubes.

Consideration of electrical currents when modelling the SOL of a tokamak plasma is important in order to calculate electric fields and ExB drift motion, as well as heat loading of the divertor targets [3] and to determine the presence of current-driven instabilities. Due to the 1-D nature of the model used, only electric fields and currents parallel to magnetic field lines are being considered. The electric field can be ascertained by using a form of Ohm's law [4]:

$$E_{\parallel}(s) = \frac{j_{\parallel}}{\sigma_{\parallel}} - \frac{0.71}{e}\frac{dkT_e}{ds} - \frac{1}{en}\frac{dp_e}{ds}, \quad (1)$$

where s is the coordinate parallel to the magnetic field lines (m), $\sigma_{\parallel}$ is the parallel electric conductivity for a fully ionized plasma ($\Omega^{-1}\,m^{-1}$), $j_{\parallel}$ is the parallel electrical current ($A\,m^{-2}$), k is Boltzmann's constant ($J\,K^{-1}$), n is particle density (m^{-3}), e is the electron charge, T_e is electron temperature (K) and p_e is the electron static pressure ($kg\,m^{-1}\,s^{-2}$). In the bulk of the SOL plasma away from divertor targets, weak parallel pressure gradients exist. This allows parallel electrical currents to influence the parallel electric field. Towards the divertor targets, strong pressure gradients dominate the parallel electric field equation as the plasma accelerates to the sound speed at the divertor plates.

Inconsistencies between the physical model in the OSM code and experimental data are reconciled by the inclusion of anomalous particle and momentum terms in the respective conservation equations. When all the physical mechanisms controlling the plasma dynamics in MAST has been accounted for, these anomalous terms are reduced.

2. Experimental constraints

In order for the OSM interpretive code to operate, experimental data is required to place boundary conditions upon the plasma solution generated to model a specific tokamak discharge. In this case, MAST shot 13,018 at 250 ms the plasma was in a

* Corresponding author. Address: Euratom/UKAEA Fusion Association, Culham Science Centre, D2/2.01 Fusion Association, Abingdon, Oxfordshire OX14 3DB, UK. Tel.: +44 1235 466401; fax: +44 1235 466379.
E-mail address: james.harrison@ukaea.org.uk (J. Harrison).

0022-3115/$ - see front matter Crown Copyright © 2009 Published by Elsevier B.V. All rights reserved.
doi:10.1016/j.jnucmat.2009.01.091

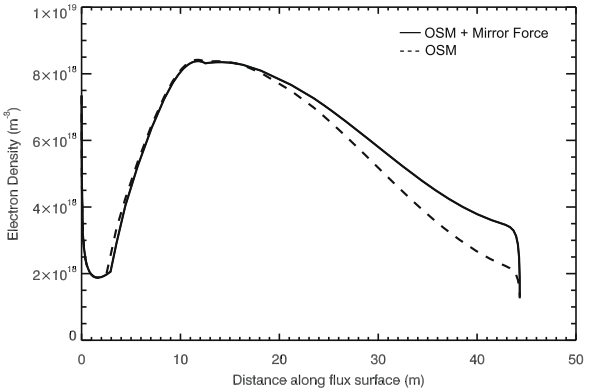

Fig. 1. Density profile with and without mirror force terms included for a flux tube 1 cm outboard of the separatrix on the low-field side.

disconnected double-null configuration, where a radial separation between the two separatrix flux tubes exists at the midplane. The core density $n_e = 2 \times 10^{19}$ m^{-3}, $T_\infty = 1.2$ keV and $I_p = 730$ kA, both targets were attached and the upper x-point was active. The SOL plasma was in a quiescent H-mode state, simplifying the plasma dynamics by reducing the effects of edge turbulence and ELMs. The magnetic field was in the 'normal' direction, i.e. the ion $B \times \nabla B$ drift is directed towards the lower divertor. The plasma is in the attached regime with respect to the four divertor target plates.

Langmuir probes embedded in the four divertor targets provided ion saturation measurements from which electron densities and temperatures were determined. Upstream electron densities and temperatures were recorded at the radial midplane by the high-resolution Thomson scattering diagnostic.

3. Magnetic mirror force

In the single-particle picture, the magnetic mirror force reduces the parallel motion of charged particles moving from a region of weaker to stronger magnetic field. In the fluid picture, the mirror force manifests itself in the form of corrections to the steady-state fluid particle and momentum conservation equations [1]:

$$\nabla_\parallel \cdot (nv) = S_p + (nv)\frac{\nabla_\parallel B}{B}, \tag{2}$$

$$\nabla_\parallel (p_e + p_i + \rho v^2 + \delta p_i) = S_{mom} + \left(\rho v^2 + \frac{3}{2}\eta\left(-\nabla_\parallel v + \frac{v}{2}\frac{\nabla_\parallel B}{B}\right)\right)\frac{\nabla_\parallel B}{B}, \tag{3}$$

where $\eta = 0.96 p_i \tau_i$ is the parallel viscosity coefficient (kg m^{-1} s^{-1}), τ_i is the ion collision time (s), v is the fluid velocity (m s^{-1}) and ρ is the mass density (kg m^{-3}), S_p is a volume particle source (m^{-3} s^{-1}) and S_{mom} is a momentum volume source (kg m^{-2} s^{-2}). The correction to the particle conservation equation is a pseudo particle source term reflecting the fact that particles tend to accumulate at mirror 'bounce points'. The dominant effect of these particle and momentum sources is to bring about a density increase as the plasma approaches the strike point (Fig. 1).

4. Parallel edge currents

4.1. Thermoelectric currents

Whenever a temperature imbalance between the ends of an electrical conductor exists, an electrical current will flow through it due to the thermoelectric effect. It has been seen that this effect is one of the dominant current-driving mechanisms in a tokamak SOL [4], especially in the region near the divertor targets where

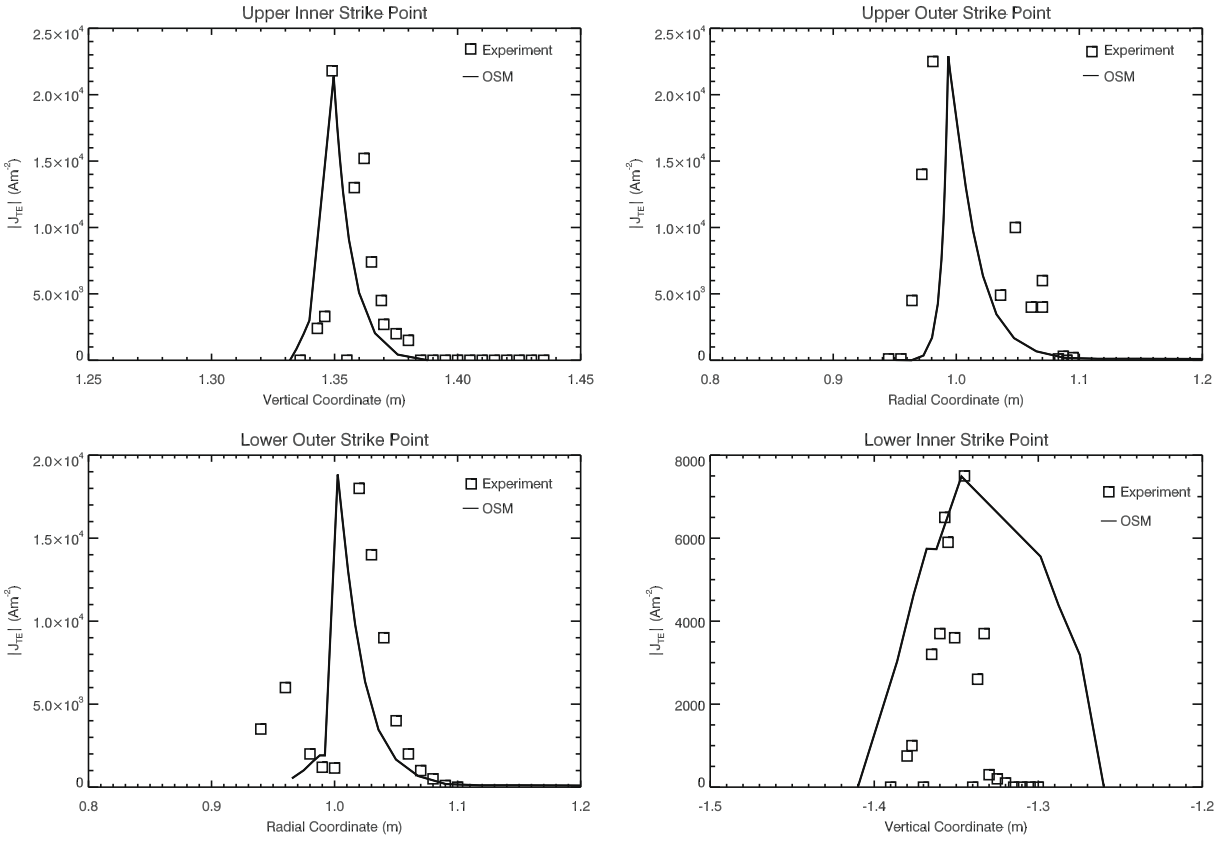

Fig. 2. Recorded and simulated thermoelectric currents.

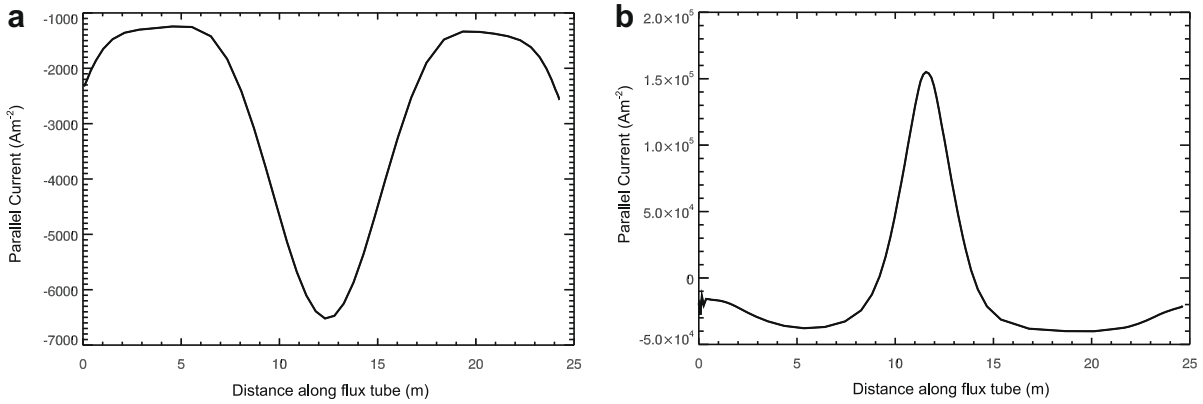

Fig. 3. (a) Parallel currents 1 cm inboard of separatrix on the high-field side. (b) Parallel currents 1 cm outboard of separatrix on the low-field side.

cross-field pressure gradients are small compared with the midplane. Following the equation derived by Stangeby [4]:

$$\hat{j}_{\parallel} = -\gamma\left[\left(\frac{1}{r_T}-1\right)(\ln(2)-0.71+\ln\alpha)+\ln\left[\frac{1+\hat{j}_{\parallel}}{(1-r_n r_T^{1/2}\hat{j}_{\parallel})^{1/r_T}}\right] - \frac{1}{kT_h}\int_h^c \frac{1}{n}\frac{dp_e}{ds_{\parallel}}ds_{\parallel}\right], \quad (4)$$

where $\hat{j}_{\parallel} = \frac{j_{\parallel}}{en_h c_{sh}}, \gamma = \frac{\bar{\sigma}_{\parallel} kT_h}{e^2 L n_h c_{sh}}, \bar{\sigma}_{\parallel} = \left[\frac{1}{L}\int_h^c \frac{ds_{\parallel}}{\sigma_{\parallel}}\right]^{-1}, \sigma_{\parallel} = \frac{e^2 n}{m_e \nu_{ei}^{mom}}, \alpha = \frac{1}{2}\left(\frac{m_i}{\pi m_e}\right)$, $r_n = \frac{n_h}{n_c}, r_T = \frac{T_h}{T_c}, n_h, T_h$ are the density and temperature at the end of the flux tube with higher temperature, whereas n_c, T_c are the density and temperature at the other end of the flux tube. c_{sh} is the acoustic sound speed at the high temperature end of the flux tube (m s^{-1}), L is the connection length between the divertor targets (m), ν_{ei}^{mom} is the electron–ion collision frequency (s^{-1}) for momentum–loss collisions. All other terms have their normal meanings. Calculations of the thermoelectric currents flowing through the SOL for the discharge simulated using the OSM model agree reasonably well with data taken from the target Langmuir probes (Fig. 2). Discrepancies between measurements and the current density predicted by the thermoelectric model are largely due to the code not reaching a satisfactory level of convergence on flux tubes located in this region.

4.2. Pfirsch–Schlüter currents

Another source of parallel currents in a tokamak SOL is required to close the divergent part of perpendicular currents, as required by the current continuity equation $\vec{\nabla}\cdot\vec{j}=0$. To simplify the model, it is assumed that the dominant cross-field current source with non-zero divergence is brought about by diamagnetic drift motion. The parallel Pfirsch–Schlüter current closes this cross-field current and the divergent part of the diamagnetic current provides a means of calculating its magnitude. The Pfirsch–Schlüter and thermoelectric currents constitute the dominant current sources in the bulk of a tokamak SOL. Using the 1-D edge current model described by Rozhansky [5], the total current density flowing parallel to a magnetic flux tube a small distance away from the separatrix can be given by:

$$j_{\parallel} = j_{\parallel}(x_0)\frac{B_T(x)}{B_T(x_0)} + \frac{B_T(x)B(x)}{B_\theta(x)}\left(\frac{1}{B^2}\frac{dp}{dr}(x) - \frac{1}{B^2}\frac{dp}{dr}(x_0)\right) - \frac{B_T(x)B(x)}{B_\theta(x)}\frac{d}{dr}\int_{x_0}^{x}\frac{1}{B^2(x')}\frac{dp}{dx'}(x')dx', \quad (5)$$

where B is the total magnetic field strength (T), B_T is the toroidal field strength, B_θ is the poloidal field strength, x is a poloidal coordinate (m), x_0 is a reference poloidal co-ordinate where the current density $j_{\parallel}$ (A m^{-2}) is known. x_0 is taken to be a divertor plate and hence $j_{\parallel}(x_0)$ is the calculated thermoelectric current flowing towards the plate. r is a radial coordinate (m) and p is the sum of the electron and ion static pressures (kg m^{-1} s^{-2}).

It can be seen that the parallel currents reverse direction on the outboard midplane (Fig. 3), this is due to a substantial increase of the integral term in Eq. (5) on the outboard side as opposed to the inboard side, due to the presence of stronger parallel pressure gradients on the outboard side. This feature of Pfirsch–Schlüter currents has been observed in other theoretical studies [5].

5. Summary and conclusions

The OSM model implemented on MAST has been extended to simulate parallel SOL currents and the effects of the magnetic mirror force in order to accurately determine the strength of parallel electric fields. The electrical current model shows good agreement with the experimental data available and the magnetic mirror force has been shown strongly to influence the density profiles in MAST discharges, as seen in previous studies [1].

Acknowledgements

This work was funded jointly by the United Kingdom Engineering and Physical Sciences Research Council and by the European Communities under the contract of Association between EURATOM and UKAEA.

References

[1] A. Kirk, W. Fundamenski, J.-W. Ahn, G. Counsell, Plasma Phys. Control. Fus. 45 (2003) 1445.
[2] S. Lisgo et al., J. Nucl. Mater. 337–339 (2005) 256.
[3] B. LaBombard et al., J. Nucl. Mater. 241–243 (1997) 149.
[4] P.C. Stangeby, The Plasma Boundary of Magnetic Fusion Devices, Institute of Physics Publishing, Bristol, 2002.
[5] V. Rozhansky et al., Nucl. Fusion 43 (2003) 614.